ENVIRONMENTAL RESEARCH
LETTERS

LETTER • OPEN ACCESS

Sulfur isotopes quantify the impact of anthropogenic activities on industrial-era Arctic sulfate in a Greenland ice core

To cite this article: Ursula A Jongebloed *et al* 2023 *Environ. Res. Lett.* **18** 074020

ENVIRONMENTAL RESEARCH
LETTERS

CrossMark

OPEN ACCESS

RECEIVED
14 February 2023

REVISED
1 June 2023

ACCEPTED FOR PUBLICATION
7 June 2023

PUBLISHED
23 June 2023

LETTER

Sulfur isotopes quantify the impact of anthropogenic activities on industrial-era Arctic sulfate in a Greenland ice core

Ursula A Jongebloed[1,*], Andrew J Schauer[2], Shohei Hattori[3,4], Jihong Cole-Dai[5], Carleigh G Larrick[5], Sara Salimi[1], Shana R Edouard[1], Lei Geng[6] and Becky Alexander[1,*]

[1] Department of Atmospheric Sciences, University of Washington, Seattle, Washington DC, United States of America
[2] Department of Earth and Space Sciences, University of Washington, Seattle, Washington DC, United States of America
[3] International Center for Isotope Effects Research, Nanjing University, Nanjing, Jiangsu, People's Republic of China
[4] School of Earth Sciences and Engineering, Nanjing University, Nanjing, Jiangsu, People's Republic of China
[5] Department of Chemistry and Biochemistry, South Dakota State University, Brookings, SD, United States of America
[6] School of Earth and Space Sciences, University of Science and Technology of China, Hefei, Anhui, People's Republic of China
[*] Authors to whom any correspondence should be addressed.

E-mail: ujongebl@uw.edu and beckya@uw.edu

Keywords: Arctic, pollution, climate, ice core, sulfate, aerosol, isotope

Supplementary material for this article is available online

Abstract

Anthropogenic sulfate aerosols are estimated to have offset 60% of greenhouse-gas-induced warming in the Arctic, a region warming four times faster than the rest of the world. However, sulfate radiative forcing estimates remain uncertain because the relative contributions from anthropogenic versus natural sources to total sulfate aerosols are unknown. Here we measure sulfur isotopes of sulfate in a Summit, Greenland ice core from 1850 to 2006 CE to quantify the contribution of anthropogenic sulfur emissions to ice core sulfate. We use a Keeling plot to determine the anthropogenic sulfur isotopic signature ($\delta^{34}S_{anthro} = +2.9 \pm 0.3$ ‰), and compare this result to a compilation of sulfur isotope measurements of oil and coal. Using $\delta^{34}S_{anthro}$, we quantify anthropogenic sulfate concentration separated from natural sulfate. Anthropogenic sulfate concentration increases to 67 ± 7% of non-sea-salt sulfate (65.1 ± 20.2 μg kg^{-1}) during peak anthropogenic emissions from 1960 to 1990 and decreases to 45 ± 11% of non-sea-salt sulfate (25.4 ± 12.8 μg kg^{-1}) from 1996 to 2006. These observations provide the first long-term record of anthropogenic sulfate distinguished from natural sources (e.g. volcanoes, dimethyl sulfide), and can be used to evaluate model characterization of anthropogenic sulfate aerosol fraction and radiative forcing over the industrial era.

1. Introduction

Sulfate aerosols have a net cooling effect on climate by scattering incoming shortwave radiation and influencing cloud microphysical and macrophysical properties (Szopa *et al* 2021). Anthropogenic emissions of SO_2, a precursor to sulfate, increased the abundance of sulfate aerosols over the industrial era, thereby imparting a significant negative radiative forcing (Shindell *et al* 2013). This increase in sulfate abundance is estimated to have offset some of the greenhouse-gas-induced warming over the industrial era, but the magnitude of this offset is the most uncertain aspect of climate modelling (Szopa *et al* 2021). A large portion of this uncertainty is caused by the unknown abundance of sulfate aerosols from natural sources because the magnitude of anthropogenic radiative forcing from aerosols is highly dependent on the preindustrial (natural) aerosol abundance (Carslaw *et al* 2013, Gettelman 2015). In other words, although inventories of historic anthropogenic SO_2 emissions are relatively certain compared to natural emissions (Carslaw *et al* 2013, McDuffie *et al* 2020), natural emissions of sulfate aerosol precursors are unknown and thus the fractions of total sulfate from natural vs. anthropogenic sources throughout the industrial era are uncertain (Carslaw *et al* 2013).

In the Arctic, which is warming four times as quickly as the rest of the world (Rantanen *et al* 2022), anthropogenic aerosols are estimated to have offset

60% of greenhouse-gas-induced warming over the industrial era, mostly due to sulfate aerosols resulting from midlatitude anthropogenic SO_2 emissions (Najafi *et al* 2015). Size-resolved sulfate aerosol measurements from Greenland ice cores confirm that anthropogenic SO_2 increased the number of small sulfate particles contributing to cloud condensation nuclei over the industrial era (Iizuka *et al* 2022). In the regions where emissions strongly affect Greenland and the North Atlantic sub-Arctic region, including North America and Europe, anthropogenic aerosol precursor emissions increased from the preindustrial through the mid-1970s, and then decreased following implementation of clean air policies in the source regions. Greenland ice core sulfate concentrations qualitatively align with these emissions trends (Moseid *et al* 2022). As a result of these trends in anthropogenic emissions of aerosol precursors, aerosol radiative cooling increased from the preindustrial into the mid-1970s and then decreased in the late 20th and early 21st centuries. The decrease in aerosol abundance contributed 1.09 °C of the 1.48 °C observed warming in the Arctic from 1976 to 2007 (Shindell and Faluvegi 2009).

However, the estimated temperature increase due to a reduction in aerosol abundance is highly dependent on unknown natural Arctic and sub-Arctic sulfate abundance, which is sourced from volcanic sulfur emissions, marine phytoplankton dimethyl sulfide (DMS) emissions, and sea-salt aerosols (Norman *et al* 1999, Patris *et al* 2002, Abbatt *et al* 2019, Jongebloed *et al* 2023). Biomass burning is not a significant source of Arctic sulfate (Breider *et al* 2014, Abbatt *et al* 2019). Sulfur isotopes can be used to determine relative contribution of anthropogenic and natural sources to total sulfate when the isotopic signatures are known and sufficiently distinct from each other (Norman *et al* 1999, 2000, Patris *et al* 2002, Wadleigh 2004, Wasiuta *et al* 2006, Jongebloed *et al* 2023). In this study we present observations of sulfur isotopes of sulfate in Greenland ice core samples and use them to quantify anthropogenic and natural sulfate over the industrial era.

2. Methods

In an ice core from Summit, Greenland collected in 2007, we measure sulfate concentration and sulfur isotopic composition of sulfate ($\delta^{34}S(SO_4{}^{2-})$) in samples selected in years between 1202 and 1980 CE without influence from large volcanic eruptions (Cole-Dai *et al* 2013, Gautier *et al* 2019) and every year from 1980 to 2006 CE. Results and discussion of anthropogenic sulfate trends in sections 3.2 and 3.3 exclude the years 1976, 1980, 1982, 1986, 1991, and 1992, which are influenced by major volcanic eruptions. Years with major volcanic eruptions prior to 1980 were not measured. Detailed methods for sample analysis are described in Jongebloed *et al* (2023). We analyze a total of 135 samples representing 184 sampled years, including one sample per decade from 1200 to 1750 CE at 1- to 2-year resolution, one sample every 4 years from 1750 to 1980 CE at 1-year resolution, and one sample each year at 1-year resolution from 1980 to 2006 CE. The uncertainty for sample SO_4^{2-} concentration measurements is ± 1.0 μg kg^{-1} and the uncertainty for $\delta^{34}S(SO_4{}^{2-})$ measurement determined by replicate analysis of whole-process standards is ± 1.2 ‰.

The isotopic composition and concentration of ice core sulfate can be used to estimate the relative contribution from each of its main sources (Norman *et al* 1999, Patris *et al* 2002, Wasiuta *et al* 2006, Jongebloed *et al* 2023), as effects of oxidation and transport on sulfur isotopic composition are minimal (Uemura *et al* 2016, Ishino *et al* 2019). The fraction of sea-salt sulfate in each sample is calculated using the mass fraction of bulk sea water $SO_4^{2-}/Na^+ = 0.25$ (Holland 1978), and sea salt contributes 2.1% of total ice core sulfate on average. The non-sea-salt sulfate ($nssSO_4^{2-}$) sulfur isotopic composition ($\delta^{34}S(nssSO_4{}^{2-})$) is calculated by subtracting out the isotopic signature of sea salt sulfate ($\delta^{34}S_{ss} = +21$ ‰; Rees *et al* 1978). In the preindustrial samples (prior to 1850), the anthropogenic contribution to sulfate concentration is assumed to be negligible, and $nssSO_4^{2-}$ originates from only DMS and volcanoes. Other natural sources of sulfate are thought to be negligible in the Arctic (Abbatt *et al* 2019, Patris *et al* 2002, Jongebloed *et al* 2023). The isotopic signature of biogenic sulfate ($\delta^{34}S_{bio}$) is well constrained at $+18.8 \pm 0.3$ ‰ and the volcanic isotopic signature ($\delta^{34}S_{volc}$) was previously estimated to be $+4.1 \pm 0.5$ ‰ (Jongebloed *et al* 2023). Consequently, preindustrial $nssSO_4^{2-}$ is the sum of biogenic and volcanic sulfate (equation (1)) and $\delta^{34}S(nssSO_4{}^{2-})$ is a weighted average of $\delta^{34}S_{bio}$ and $\delta^{34}S_{volc}$ (equation (2)):

$$f_{bio} + f_{volc} = 1 \tag{1}$$

$$f_{bio}\delta^{34}S_{bio} + f_{volc}\delta^{34}S_{volc} = \delta^{34}S(nssSO_4^{2-}) \tag{2}$$

where f_{bio} is the biogenic fraction and f_{volc} is the volcanic fraction of total non-sea-salt sulfate.

In the post-1850 samples, we assume that $nssSO_4^{2-}$ is the sum of anthropogenic, biogenic, and volcanic sulfate (equation (3)) and that $\delta^{34}S(nssSO_4{}^{2-})$ results from a weighted average of $\delta^{34}S_{anthro}$, $\delta^{34}S_{bio}$, and $\delta^{34}S_{volc}$ (equation (4)):

$$f_{anthro} + f_{bio} + f_{volc} = 1 \tag{3}$$

$$f_{anthro}\delta^{34}S_{anthro} + f_{bio}\delta^{34}S_{bio} + f_{volc}\delta^{34}S_{volc} = \delta^{34}S(nssSO_4^{2-}) \tag{4}$$

where f_{anthro} is the fraction of anthropogenic sulfate in the sample and $\delta^{34}S_{anthro}$ is the anthropogenic sulfur isotopic source signature. We estimate the anthropogenic sulfur isotopic source signature ($\delta^{34}S_{anthro}$)

using two methods: a Keeling plot over the post-1850 ice core samples (Keeling 1958, 1989, Pataki et al 2003) and statistical analysis of direct δ^{34}S measurements of coal and oil. Results of both methods are discussed in section 3.1.

The distinct isotopic composition of biogenic sulfur compared to that of other sources (Norman et al 1999, Patris et al 2002, Wasiuta et al 2006, Ghahremaninezhad et al 2016) and prior quantification of volcanic sulfate concentrations during the preindustrial era (Jongebloed et al 2023) quantify how much anthropogenic emissions perturbed sulfate aerosol abundance from 1850 to 2006 in years without major volcanic eruptions. Due to the similarity in $\delta^{34}S_{anthro}$ (+2.9 ± 0.3 ‰, see section 3.1) and $\delta^{34}S_{volc}$ (+4.1 ± 0.5 ‰), volcanic and anthropogenic sulfate cannot be separated using $\delta^{34}S(nssSO_4{}^{2-})$ measurements. Additionally, the likely underestimate of global volcanic sulfur emissions from satellite observations (Carn et al 2015, 2017, Fischer et al 2019, Jongebloed et al 2023) preclude the use of volcanic sulfur emissions to constrain ice core volcanic sulfate concentrations over the industrial era. We therefore assume volcanic sulfate concentrations during the industrial era are equal to the median of preindustrial volcanic sulfate concentration (figure S1) and subtract the contribution of volcanic sulfur from $\delta^{34}S(nssSO_4{}^{2-})$ based on this assumption. We also assume volcanic sulfate concentrations ±2 standard deviations around the mean preindustrial volcanic sulfate concentration (figure S1) to provide a range of anthropogenic sulfate concentrations considering the unknown volcanic sulfate contribution. It is difficult to use other measurements to examine volcanic emissions because compounds emitted by volcanoes (e.g. sulfur, carbon dioxide, trace metals) are also emitted during anthropogenic activities (e.g. fossil fuel burning and metal smelting). With these assumptions, we estimate f_{anthro} from equations (3) and (4), and the concentration of anthropogenic sulfate is calculated in each sample (equation (5)):

$$\left[SO_4^{2-}\right]_{anthro} = f_{anthro} \cdot \left[nssSO_4^{2-}\right] \quad (5)$$

where $[SO_4^{2-}]_{anthro}$ is anthropogenic sulfate concentration. The range in f_{anthro} based on the 2.5th–97.5th percentile of volcanic sulfate concentrations in the preindustrial is also estimated in each ice core sample.

3. Results and discussion

3.1. Determination of anthropogenic sulfur isotopic signature

Figure 1 shows a Keeling plot of the post-1850 ice core samples in years without large volcanic eruptions. The resulting isotopic source signature for anthropogenic sulfur emissions is $\delta^{34}S_{anthro}$ = +2.9 ± 0.3 ‰, where the signature is determined by the geometric mean intercept of $1/[nssSO_4{}^{2-}]$ vs. $\delta^{34}S(nssSO_4{}^{2-})$ to correct for the negative slope bias in ordinary linear regression (Angleton and Bonham 1995, Laws 1997, Pataki et al 2003) and the uncertainty is determined by the standard error of the intercept as recommended by Pataki et al (2003).

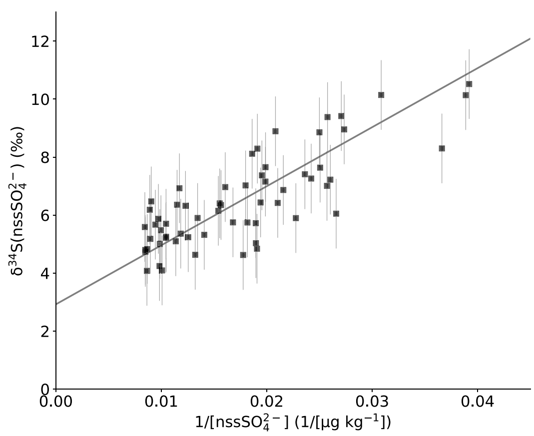

Figure 1. Determination of $\delta^{34}S_{anthro}$ using a Keeling plot. Black symbols indicate the one-year samples collected once per four years between 1850 and 1980 and one-year samples collected every year between 1980 and 2006. Volcanic eruption samples (see figure 3) are excluded. Error bars represent analytical error of sulfur isotope measurements based on replicate analysis of whole-process standards. The geometric mean regression intercept is $\delta^{34}S_{anthro}$ = +2.9 ± 0.3 ‰, where error is estimated from the standard error of the intercept.

We compare $\delta^{34}S_{anthro}$ = +2.9 ± 0.3 ‰ determined by the Keeling plot in figure 1 to direct measurements of coal and oil sulfur isotopic composition from prior studies summarized in table S1 and figure S2. We do not include δ^{34}S measurements of precipitation or aerosols because these samples include influence from non-anthropogenic sources (e.g. DMS). The δ^{34}S measurements are organized by location (country or region), fossil fuel type (coal vs. oil), and fossil fuel source. In general, when multiple measurements represent the same fossil fuel source (e.g. δ^{34}S measurements of sulfur in oil from the same well), they are combined into one 'sample.' We compile 1969 measurements of fossil fuel δ^{34}S into 1012 samples, including 258 coal samples and 754 oil samples.

Figure S2 shows the distribution of δ^{34}S of the 1012 samples summarized in table S1. The sample δ^{34}S measurements range from −35 to +33 ‰ with a mean of +3.4 ‰ and a standard deviation of ± 9.6 ‰. We assume that the $\delta^{34}S_{anthro}$ in the ice core is a mass-weighted mean of many isotopic signatures from many individual anthropogenic sources and therefore analyze the mean statistics of the compilation shown in figure 1 to estimate $\delta^{34}S_{anthro}$. We estimate that the mean $\delta^{34}S_{anthro}$ = +3.4 ± 0.3 ‰, where the uncertainty is the standard error of

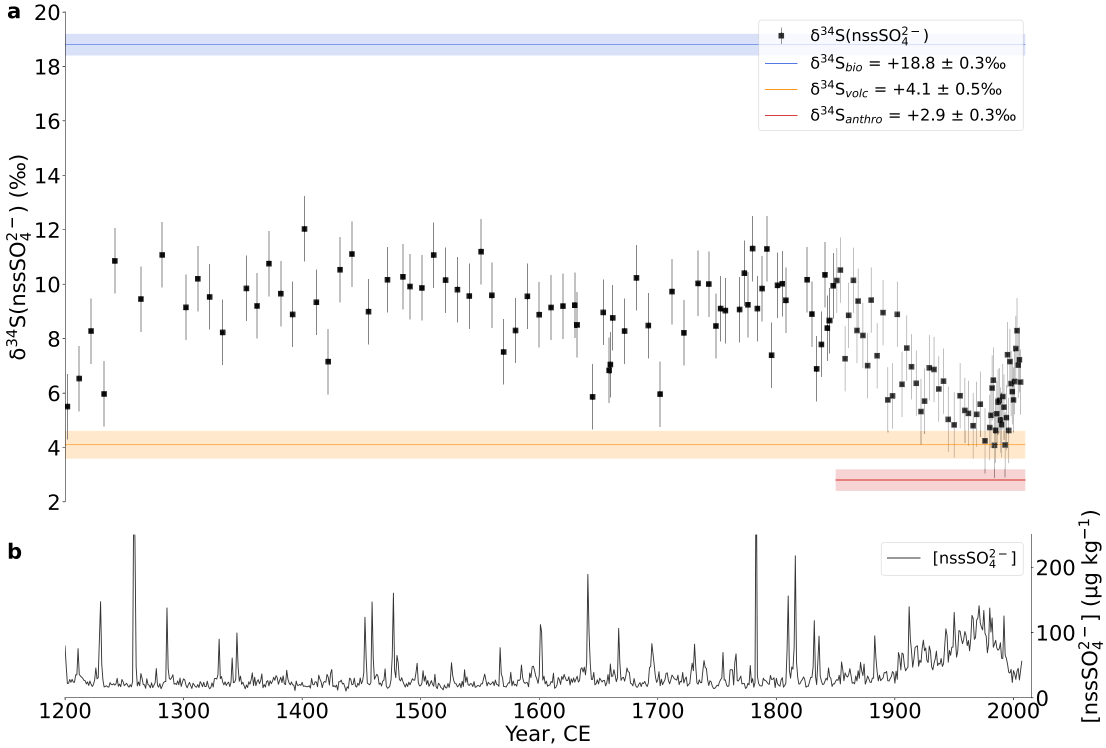

Figure 2. (a) Decadal and sub-decadal ice core $\delta^{34}S(nssSO_4{}^{2-})$ (‰, black symbols) Thick colored bars show the isotopic signatures of biogenic sulfur ($\delta^{34}S_{bio} = +18.8 \pm 0.3$ ‰), volcanic sulfur ($\delta^{34}S_{volc} = +4.1 \pm 0.5$ ‰), and anthropogenic sulfur ($\delta^{34}S_{anthro} = +2.9 \pm 0.3$ ‰). Error in $\delta^{34}S(nssSO_4{}^{2-})$ measurements is estimated based on replicate analysis of whole-process standards. (b) Annual mean $nssSO_4^{2-}$ concentration (μg kg^{-1}, gray line) from Cole-Dai *et al* (2013). Large peaks in $nssSO_4^{2-}$ concentration prior to 1850 are attributed to volcanic eruptions (Cole-Dai *et al* 2013).

the mean determined by a bootstrapping method (re-sampling the 1012 samples 1000 times with replacement and taking the mean of each re-sample (Wasserman 2004)), which is an appropriate method for determining the variance of a population that cannot be assumed to be normally distributed. Assuming the measurements are normally distributed, the standard error of the mean is also estimated to be ±0.3 ‰.

The value of $\delta^{34}S_{anthro} = +3.4 \pm 0.3$ ‰ determined by statistical analysis of the compiled direct measurements of fossil fuel $\delta^{34}S$ is similar to $\delta^{34}S_{anthro} = +2.9 \pm 0.3$ ‰ from our Keeling plot in figure 1. $\delta^{34}S_{anthro} = +2.9 \pm 0.3$ ‰ and $\delta^{34}S_{anthro} = +3.4 \pm 0.3$ ‰ both align with prior estimates of $\delta^{34}S_{anthro} = +3 \pm 3$ ‰ (Nriagu *et al* 1991, Barrie *et al* 1992, Norman *et al* 1999, Li *et al* 2018). This estimate for $\delta^{34}S_{anthro}$ is similar to measured $\delta^{34}S$ of aerosols in regions dominated by anthropogenic SO_2 emissions (Fan *et al* 2020, Nriagu *et al* 1991, Barrie *et al* 1992, Li *et al* 2018), suggesting that minimal fractionation due to transport and oxidation. However, as discussed in Text S1, the compilation in table S1 and figure S2 is not an unbiased representation of anthropogenic sulfur in the Summit air mass source region. Thus, we perform calculations with the signature $\delta^{34}S_{anthro} = +2.9 \pm 0.3$ ‰ determined by the Keeling plot because this method is more likely to be representative of the anthropogenic sulfur reaching the ice core.

3.2. Ice core anthropogenic sulfate concentration and fraction

Figure 2 shows ice core measurements of $nssSO_4^{2-}$ and $\delta^{34}S(nssSO_4{}^{2-})$ in samples from 1200 to 2006 CE. Prior to 1980, years with major volcanic eruptions are not measured. After 1980, years with major volcanic eruptions are marked with blue symbols and excluded from discussion of statistics (e.g. post-1980 mean anthropogenic sulfate concentrations). The concentration of $nssSO_4^{2-}$ more than triples from the preindustrial mean of 29.0 ± 7.7 μg kg^{-1} to a peak concentration of 114.7 ± 15.8 μg kg^{-1} between 1970 and 1980 CE (figure 2(b)), aligning with observations from Mayewski *et al* (1986). The opposite pattern is seen in $\delta^{34}S(nssSO_4{}^{2-})$, which decreases from +9.2 ± 1.4 ‰ in the preindustrial to a low of +4.9 ± 0.6 ‰ from the 1970s through the late 1990s, and then increases to +7.3 ± 0.6 ‰ from 2002 to 2006 (figure 2(a)). The pattern in $\delta^{34}S(nssSO_4{}^{2-})$ reflects a shift from natural sulfate sources in the preindustrial ($\delta^{34}S_{bio} = +18.8 \pm 0.3$ ‰ and $\delta^{34}S_{volc} = +4.1 \pm 0.5$ ‰) to natural sulfate plus variable contribution of anthropogenic sulfur ($\delta^{34}S_{anthro} = +2.9 \pm 0.3$ ‰; figure 1), causing a decreasing and then increasing trend in ice core

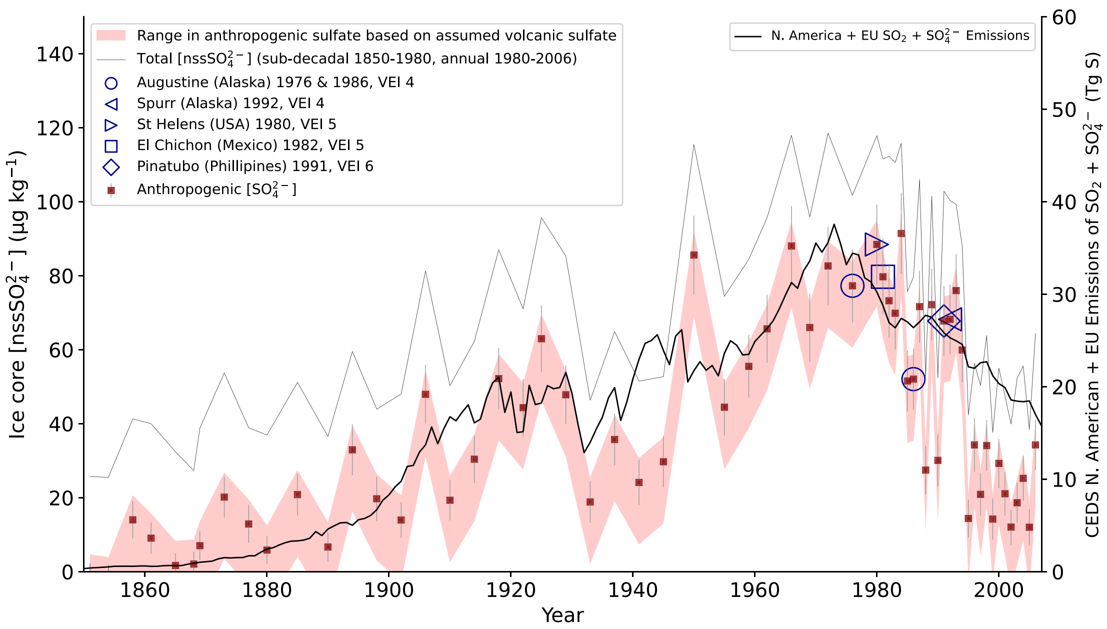

Figure 3. Concentrations of anthropogenic sulfate from 1850 to 2006 (μg kg^{-1}, red squares). Error bars were determined by propagating the uncertainty in isotopic source signatures and sample measurement error. Red shaded region shows the range in possible anthropogenic sulfate concentrations based on volcanic sulfate concentrations from the 2.5th and 97.5th percentile of the preindustrial volcanic sulfate concentration distribution. Gray line shows total nssSO$_4^{2-}$ concentrations (μg kg^{-1}). Between 1850 and 1980, one sample per four years were selected in years without major volcanic eruptions. Every year between 1980 and 2006 was sampled, including years with volcanic eruptions. Blue shapes outline years with eruptions with volcanic explosivity index (VEI) $>$ 4 from around the world and years with eruptions with VEI $>$ 3 in areas near the Arctic (i.e. Alaska, Iceland, and Kamchatka) (Venzke 2013). Anthropogenic sulfate concentrations from 1850 to 1854 are negligible. The sum of North American and European sulfur ($SO_2 + SO_4{}^{2-}$) emissions from the Community Emission Data System (CEDS) inventory are shown as a thick black line.

δ^{34}S(nssSO$_4{}^{2-}$) as anthropogenic emissions increase through the 1970s and then decrease following implementation of clean air policies (McDuffie *et al* 2020).

Figure 3 shows ice core anthropogenic sulfate concentrations from 1850 to 2006 CE and anthropogenic $SO_2 + SO_4{}^{2-}$ emissions from North America and the European Union (McDuffie *et al* 2020), which are the regions contributing ~90% of anthropogenic sulfate at Summit over the past century (Moseid *et al* 2022). Emissions from North America and Europe increased from a mean of 8 Tg S yr^{-1} from 1850 to 1900 to 20 Tg yr^{-1} in 1930. North American and European SO_2 emissions increased to a mean of 69 Tg S yr^{-1} from 1960 to 1990. North American SO_2 emissions decrease after 1973, earlier than the European decrease starting in 1979. Clean air policies in North America and Europe decreased emissions to a mean of 31 Tg S yr^{-1} from 1995 to 2006. Anthropogenic ice core sulfate concentrations increase from a mean of 12.8 $\pm$ 8.9 μg kg^{-1} from 1858 to 1900 (we disregard samples from 1850 to 1854 because anthropogenic sulfate values are indistinguishable from zero) to a mean of 65.1 $\pm$ 20.2 μg kg^{-1} from 1962 to 1990. A decrease in anthropogenic sulfate concentration from 1930 to 1940 and subsequent renewed growth reflects a decline in fossil fuel burning during the Great Depression and renewed growth during and after World War II. As emissions decreased in North America and Europe after 1970, concentrations decreased to a mean of 25.4 $\pm$ 12.8 μg kg^{-1} from 1995 to 2006 (near the top of the core). Due to volcanic eruptions in the early 1980s and 1990s, the beginning of the decrease in anthropogenic sulfate concentrations is difficult to discern as aligning with the North American vs. European decrease in SO_2 emissions. Decreasing ice core anthropogenic sulfate concentrations (figure 3) align with decreasing sulfate aerosol concentration trends in sites around the Arctic (Schmale *et al* 2022). Anthropogenic sulfate concentrations are correlated with North American $SO_2 + SO_4{}^{2-}$ emissions alone ($r^2 = 0.60$) from 1850 to 2006, European $SO_2 + SO_4{}^{2-}$ emissions alone ($r^2 = 0.68$) from 1850 to 2006, and with the sum of North American and European $SO_2 + SO_4{}^{2-}$ emissions ($r^2 = 0.68$).

Figure 4 shows ice core f_{anthro} from 1850 to 2006 CE. Ice core f_{anthro} is on average 28 $\pm$ 15% from 1854 to 1900, 67 $\pm$ 7% from 1960 to 1990 (years of highest anthropogenic SO_2 emissions; McDuffie *et al* 2020), and 45 $\pm$ 11% from 1995 to 2006 (near the top of the ice core). The natural nssSO$_4^{2-}$ fraction ($f_{natural} = f_{bio} + f_{volc} = 1 - f_{anthro}$) is assumed to be 100% of nssSO$_4^{2-}$ during the preindustrial, is 33 $\pm$ 7%

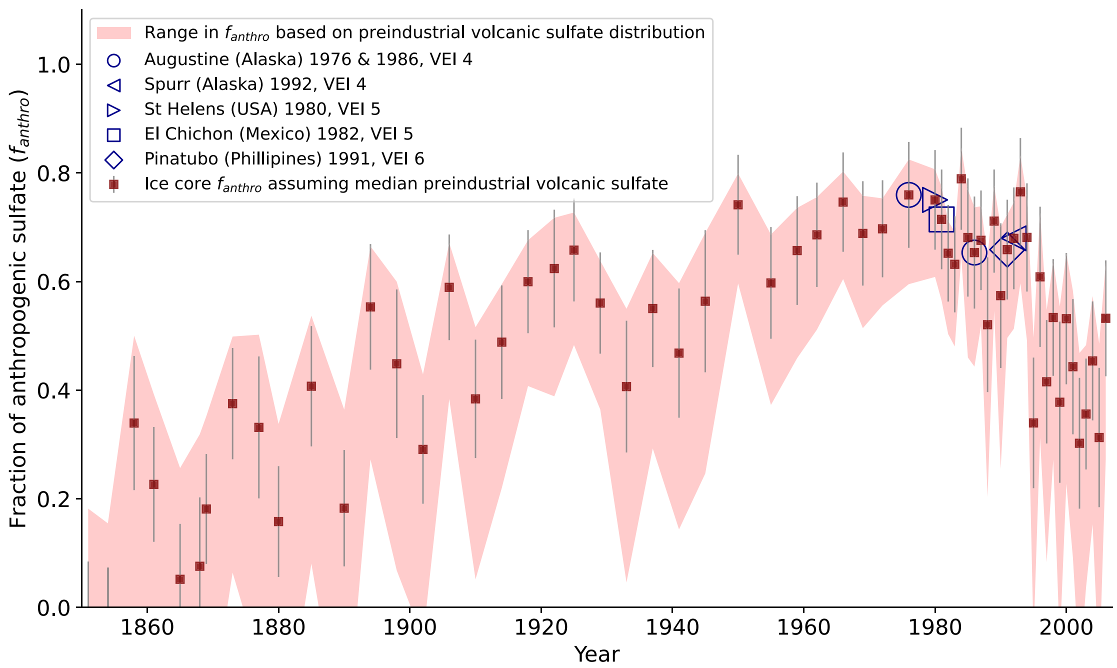

Figure 4. Fraction of anthropogenic sulfate concentration (f_{anthro}) in total non-sea-salt sulfate. Error bars were determined by propagating the uncertainty in isotopic source signatures and sample measurement error. Red shaded region and blue shapes are the same as in figure 3. Values of f_{anthro} from 1850 to 1854 are approximately zero.

from 1960 to 1990, and 55 ± 11% from 1996 to 2006. For 35 of the 61 years sampled over the industrial era, including the 35 years sampled from 1850 to 1980 and the 26 years sampled from 1980 to 2006, anthropogenic sulfate is more than half of the total $nssSO_4^{2-}$ in the ice core (figure 4). Figure 4 also shows that natural sulfate aerosols become increasingly important as anthropogenic emissions decline following implementation of clean air policies in North America, and natural sulfate begins to dominate over anthropogenic sulfate at the end of the ice core record (1996–2006).

The estimated f_{anthro} in figure 4 varies by 41% on average depending on the assumed volcanic sulfate concentration, where we assume a conservative range of ±2 standard deviations around the mean preindustrial volcanic sulfate concentration. The estimated f_{anthro} assuming the median preindustrial volcanic sulfate concentration (from here on 'median-based f_{anthro}') is on average 12 ± 5% lower than the upper-end estimate of f_{anthro} (assuming industrial-era volcanic sulfate concentrations are equal to the 2.5th percentile from the preindustrial, figure S1), whereas the difference between the median-based f_{anthro} and the lower end estimate for f_{anthro} (assuming industrial-era volcanic sulfate concentrations are equal to the 97.5th percentile from the preindustrial, figure S1) is on average 29 ± 18%. The relatively small difference between the median-based anthropogenic concentration and the upper-end estimate is due to the positive skew of preindustrial volcanic sulfate concentrations around the mean and median. This positive skew in the preindustrial volcanic sulfate concentrations and corresponding positively skewed assumed industrial-era volcanic sulfate concentrations results in the median-based f_{anthro} near the upper end of its possible range. In other words, this dataset provides an upper bound on f_{anthro}.

3.3. Comparison of ice-core anthropogenic sulfate concentrations with emissions

Anthropogenic sulfate concentration trends qualitatively align with anthropogenic emissions from regions affecting Greenland, primarily North America and Europe (Moseid *et al* 2022), throughout the industrial era (figure 3). We note that North American and European SO_2 emissions from 1996 to 2006 are similar to emissions from 1918 to 1930 (35 Tg S yr^{-1} and 33 Tg S yr^{-1}, respectively), but anthropogenic sulfate concentration is 23.3 μg kg^{-1} from 1996 to 2006 compared to 51.8 μg kg^{-1} from 1918 to 1930. Similar discrepancies between emissions and anthropogenic sulfate concentrations occur earlier in the time series (e.g. 1930–1950; however, this period was not sampled annually), and the discrepancy between emissions and sulfate concentrations between 1996 and 2006 is not statistically significant ($p = 0.013$) due to the low number of samples from 1918 to 1930 ($N = 5$). We therefore do not discuss this discrepancy further.

A modeling study suggested that increasing East and South Asian anthropogenic SO_2 emissions began to influence Greenland in the late 20th and early 21st centuries in modelled sulfate deposition (Moseid *et al*

2022). However, anthropogenic ice core sulfate concentrations do not show an increase during the time period of increasing East Asian emissions (figure 3). Anthropogenic sulfate concentration decline faster than the decrease in North American and European emissions (figure 3). However, the trends presented here represent a limited number of samples from only one ice core location and more investigation is required to quantify trends after 2006 in Summit, Greenland and the rest of the Arctic.

Due to the similar isotopic signatures of volcanic and anthropogenic sulfur, the assumption of constant volcanic sulfate concentrations based on the preindustrial distribution causes the appearance of high anthropogenic sulfate concentrations during years of anomalously high volcanic emissions. For example, in the years 1991–1993, anthropogenic sulfate concentrations are likely overestimated due to influence from the eruption of Mt. Pinatubo in June 1991, which injected about 9 Tg S into the atmosphere and increased atmospheric sulfate aerosol abundance for the following 2–3 years (Guo *et al* 2004). We mark years with volcanic eruptions that might cause a high bias in anthropogenic sulfate concentrations in figure 3 based on the Global Volcano Program archive of eruptions (Venzke 2013). Similarly, our ice core measurements cannot quantify the impact of volcanic eruptions on sulfate aerosol abundance during the industrial era because anthropogenic sulfate influences the quantity of total $nssSO_4^{2-}$ and anthropogenic and volcanic sulfate have similar isotopic signatures.

The similarity in volcanic and anthropogenic sulfur isotopic signatures also creates a large range in estimated f_{anthro} and anthropogenic sulfate concentration depending on the assumed volcanic sulfate concentration. However, as demonstrated in figure 4, the positive skew in the preindustrial volcanic sulfate concentrations causes our estimates of f_{anthro} to provide an upper bound on anthropogenic contribution to ice core sulfate over the industrial era.

4. Conclusions

Our record of sulfur isotopic composition of sulfate in a Summit, Greenland ice core provides the first estimate of anthropogenic sulfate concentration separated from natural sulfate over the industrial era. Due to rising anthropogenic SO_2 emissions from the preindustrial to the 1970s, anthropogenic sulfate increased to 67 ± 7% of total $nssSO_4^{2-}$ on average from 1962 to 1990 (excluding years with major volcanic eruptions). Following clean air policies and declining emissions in North America and Europe, anthropogenic sulfate declined in the late 20th and early 21st centuries, and anthropogenic sulfate concentration is similar to natural sulfate at the end of the record (1996–2006 mean $f_{anthro} = 45 \pm 11\%$ and $f_{volc} + f_{bio} = 55 \pm 11\%$; excluding years with major volcanic eruptions).

In this study, we provide the first long-term quantification of anthropogenic ice core sulfate fraction and concentration. Future combined measurements of oxygen and sulfur isotopes could provide information about changes in both the magnitude of anthropogenic sulfate and how it influences pH-dependent sulfate formation chemistry (Alexander *et al* 2004, Hattori *et al* 2021). Quantifying anthropogenic sulfate fraction and abundance is critical for estimating sulfate aerosol radiative forcing. These results provide an upper-bound estimate for the anthropogenic fraction of industrial-era sulfate deposited in Summit, Greenland. This dataset can be compared to high resolution global modelling of the anthropogenic perturbation to sulfate deposition over Summit, Greenland to constrain model estimates of anthropogenic perturbation to sulfate aerosol abundance over the industrial era and implications for radiative forcing.

Data availability statement

All ice core data are available in the National Science Foundation (NSF) Arctic Data Center (https://doi.org/10.18739/A26T0GX7K) and here as Supplementary Data File 1. The coal and oil sulfur isotope measurement data compiled from previous studies are available in Supplementary Data File 2.

Acknowledgments

U J and B A acknowledge NSF Grants PLR 1904128 and AGS 1702266. S H acknowledges JSPS KAKENHI (20H04305 and 18H05292), support from National Natural Science Foundation of China (Excellent Young Scientists Fund Program (Overseas)), and start-up funding from Nanjing University. J C-D acknowledges NSF Grant PLR 0612461 and PLR 1904142. L G acknowledges support from National Natural Science Foundation of China (41822605 and 41871051).

Conflict of interest

There are no known no conflicts of interest.

ORCID iDs

Ursula A Jongebloed https://orcid.org/0000-0002-9482-4857
Andrew J Schauer https://orcid.org/0000-0002-5941-5396
Shohei Hattori https://orcid.org/0000-0002-4438-5462
Jihong Cole-Dai https://orcid.org/0000-0003-0921-5916

Lei Geng https://orcid.org/0000-0003-2175-2538
Becky Alexander https://orcid.org/0000-0001-9915-4621

References

Abbatt J P D *et al* 2019 Overview paper: new insights into aerosol and climate in the Arctic *Atmos. Chem. Phys.* **19** 2527–60

Alexander B, Savarino J, Kreutz K J and Thiemens M H 2004 Impact of preindustrial biomass-burning emissions on the oxidation pathways of tropospheric sulfur and nitrogen *J. Geophys. Res. Atmos.* **109**

Angleton G M and Bonham C D 1995 Least squares regression vs. geometric mean regression for ecotoxicology studies *Appl. Math. Comput.* **72** 21–32

Barrie L, Ahier B, Bottenheim J, Nikit H and Nriagu J 1992 Atmospheric methane and sulphur compounds at a remote central Canadian location *Atmos. Environ.* **26** 907–25

Breider T J, Mickley L J, Jacob D J, Wang Q, Fisher J A, Chang R Y W and Alexander B 2014 Annual distributions and sources of Arctic aerosol components, aerosol optical depth, and aerosol absorption *J. Geophys. Res.* **119** 4107–24

Carn S A, Fioletov V E, Mclinden C A, Li C and Krotkov N A 2017 A decade of global volcanic SO_2 emissions measured from space *Sci. Rep.* **7** 44095

Carn S A, Yang K, Prata A J and Krotkov N A 2015 Extending the long-term record of volcanic SO_2 emissions with the ozone mapping and profiler suite nadir mapper *Geophys. Res. Lett.* **42** 925–32

Carslaw K S *et al* 2013 Large contribution of natural aerosols to uncertainty in indirect forcing *Nature* **503** 67–71

Cole-Dai J, Ferris D G, Lanciki A L, Savarino J, Thiemens M H and McConnell J R 2013 Two likely stratospheric volcanic eruptions in the 1450s C.E. found in a bipolar, subannually dated 800 year ice core record *J. Geophys. Res. Atmos.* **118** 7459–66

Fan M-Y, Zhang Y-L, Lin Y-C, Li J, Cheng H, An N, Sun Y, Qiu Y, Cao F and Fu P 2020 Roles of sulfur oxidation pathways in the variability in stable sulfur isotopic composition of sulfate aerosols at an urban site in Beijing, China *Environ. Sci. Technol. Lett.* **7** 883–8

Fischer T P *et al* 2019 The emissions of CO_2 and other volatiles from the world's subaerial volcanoes *Sci. Rep.* **9** 1–11

Gautier E, Savarino J, Hoek J, Erbland J, Caillon N, Hattori S, Yoshida N, Albalat E, Albarede F and Farquhar J 2019 2600 years of stratospheric volcanism through sulfate isotopes *Nat. Commun.* **10** 466

Gettelman A 2015 Putting the clouds back in aerosol-cloud interactions *Atmos. Chem. Phys.* **15** 12397–411

Ghahremaninezhad R, Norman A L, Abbatt J P D, Levasseur M and Thomas J L 2016 Biogenic, anthropogenic and sea salt sulfate size-segregated aerosols in the Arctic summer *Atmos. Chem. Phys.* **16** 5191–202

Guo S, Bluth G J S, Rose W I, Watson I M and Prata A J 2004 Re-evaluation of SO_2 release of the 15 June 1991 Pinatubo eruption using ultraviolet and infrared satellite sensors *Geochem. Geophys. Geosyst.* **5** 1–31

Hattori S *et al* 2021 Isotopic evidence for acidity-driven enhancement of sulfate formation after SO_2 emission control *Sci. Adv.* **7** eabd4610

Holland H D 1978 *The Chemistry of the Atmosphere and Oceans* (New York: Wiley)

Iizuka Y, Uemura R, Matsui H, Oshima N, Kawakami K, Hattori S, Ohno H and Matoba S 2022 High flux of small sulfate aerosols during the 1970s reconstructed from the SE-dome ice core in Greenland *J. Geophys. Res.* **127** e2022JD036880

Ishino S, Hattori S, Savarino J, Legrand M, Albalat E, Albarede F, Preunkert S, Jourdain B and Yoshida N 2019 Homogeneous sulfur isotope signature in East Antarctica and implication for sulfur source shifts through the last glacial-interglacial cycle *Sci. Rep.* **9** 12378

Jongebloed U A *et al* 2023 Underestimated passive volcanic sulfur degassing implies overestimated anthropogenic aerosol forcing *Geophys. Res. Lett.* **50** e2022GL102061

Keeling C D 1958 The concentration and isotopic abundances of atmospheric carbon dioxide in rural areas *Geochim. Cosmochim. Acta* **13** 322

Keeling C D, Bacastow R B, Carter A F, Piper S C, Whorf T P, Heimann M, Mook W G and Roeloffzen H 1989 A three-dimensional model of atmospheric CO_2 transport based on observed winds: 1 *Analysis of Observational Data Aspects of Climate Variability in the Pacific and the Western Americas* vol 55, ed D H Peterson (Washington, DC: AGU) pp 165–236

Laws E 1997 *Mathematical Methods for Oceanographers* (New York: Wiley)

Li J, Michalski G, Davy P, Harvey M, Katzman T and Wilkins B 2018 Investigating source contributions of size-aggregated aerosols collected in Southern Ocean and Baring Head, New Zealand using sulfur isotopes *Geophys. Res. Lett.* **45** 3717–27

Mayewski P A, Lyons W B, Spencer M J, Twickler M, Dansgaard W, Koci B, Davidson C I and Honrath R E 1986 Sulfate and nitrate concentrations from a South Greenland ice core *Science* **232** 975–7

McDuffie E E, Smith S J, O'Rourke P, Tibrewal K, Venkataraman C, Marais E A, Zheng B, Crippa M, Brauer M and Martin R V 2020 A global anthropogenic emission inventory of atmospheric pollutants from sector-and fuel-specific sources (1970–2017): an application of the community emissions data system (CEDS) *Earth Syst. Sci. Data* **12** 3413–42

Moseid K O, Schulz M, Eichler A, Schwikowski M, McConnell J R, Olivié D, Criscitiello A S, Kreutz K J and Legrand M 2022 Using ice cores to evaluate CMIP6 aerosol concentrations over the historical era *J. Geophys. Res.* **127** e2021JD036105

Najafi M R, Zwiers F W and Gillett N P 2015 Attribution of Arctic temperature change to greenhouse-gas and aerosol influences *Nat. Clim. Change* **5** 246–9

Norman A L, Barrie L A, Toom-Sauntry D, Sirois A, Krouse H R, Li S M and Sharma S 1999 Sources of aerosol sulphate at alert: apportionment using stable isotopes *J. Geophys. Res.* **104** 11619–31

Nriagu J O, Coker R D and Barrie L A 1991 Origin of sulphur in Canadian Arctic haze from isotope measurements *Nature* **349** 142–5

Pataki D E, Ehleringer J R, Flanagan L B, Yakir D, Bowling D R, Still C J, Buchmann N, Kaplan J O and Berry J A 2003 The application and interpretation of Keeling plots in terrestrial carbon cycle research *Glob. Biogeochem. Cycles* **17** 1022

Patris N, Delmas R J and Jouzel J 2000 Isotopic signatures of sulfur in shallow Antarctic ice cores *J. Geophys. Res. Atmos.* **105** 7071–8

Patris N, Delmas R J, Legrand M, de Angelis M, Ferron F A, Stiévenard M and Jouzel J 2002 First sulfur isotope measurements in central Greenland ice cores along the preindustrial and industrial periods *J. Geophys. Res.* **107** ACH 6-1–11

Rantanen M, Karpechko A Y, Lipponen A, Nordling K, Hyvärinen O, Ruosteenoja K, Vihma T and Laaksonen A 2022 The Arctic has warmed nearly four times faster than the globe since 1979 *Commun. Earth Environ.* **3** 168

Rees C E, Jenkins W J and Monster J 1978 The sulphur isotopic composition of ocean water sulphate* *Geochim. Cosmochim. Acta* **42** 377–81

Schmale J *et al* 2022 Pan-Arctic seasonal cycles and long-term trends of aerosol properties from 10 observatories *Atmos. Chem. Phys.* **22** 3067–96

Shindell D T *et al* 2013 Radiative forcing in the ACCMIP historical and future climate simulations *Atmos. Chem. Phys.* **13** 2939–74

Shindell D and Faluvegi G 2009 Climate response to regional radiative forcing during the twentieth century *Nat. Geosci.* **2** 294–300

Szopa S *et al* 2021 Short-lived climate forcers *Climate Change 2021: The Physical Science Basis. Contribution of Working Group I to the Sixth Assessment Report of the Intergovernmental Panel on Climate Change* (New York: Cambridge University Press) pp 817–922

Uemura R, Masaka K, Fukui K, Iizuka Y, Hirabayashi M and Motoyama H 2016 Sulfur isotopic composition of surface snow along a latitudinal transect in East Antarctica *Geophys. Res. Lett.* **43** 5878–85

Venzke E 2013 Global Volcanism Program (Washington, DC: Smithsonian Institution) (https://doi.org/10.5479/si.GVP.VOTW5-2022.5.0)

Wadleigh M A 2004 Sulphur isotopic composition of aerosols over the western North Atlantic Ocean *Can. J. Fish. Aquat. Sci.* **61** 817–25

Wasiuta V, Norman A-L and Marshall S 2006 Spatial patterns and seasonal variation of snowpack sulphate isotopes of the Prince of Wales Icefield, Ellesmere Island, Canada *Ann. Glaciol.* **43** 390–6

Wasserman L 2004 *The Bootstrap All of Statistics* (Berlin: Springer) pp 107–18